Effects of Excluded Surface Area and Adsorbate Clustering on Surface Adsorption of Proteins. II. Kinetic Models

Allen P. Minton
Section on Physical Biochemistry, Laboratory of Biochemistry and Genetics, National Institute of Diabetes and Digestive and Kidney Diseases, National Institutes of Health, Bethesda, Maryland 20892-0830 USA

ABSTRACT Models for equilibrium surface adsorption of proteins have been recently proposed (Minton, A. P., 2000. *Biophys. Chem.* 86:239–247) in which negative cooperativity due to area exclusion by adsorbate molecules is compensated to a variable extent by the formation of a heterogeneous population of monolayer surface clusters of adsorbed protein molecules. In the present work this concept is extended to treat the kinetics of protein adsorption. It is postulated that clusters may grow via two distinct kinetic pathways. The first pathway is the diffusion of adsorbed monomer to the edge of a preexisting cluster and subsequent accretion. The second pathway consists of direct deposition of a monomer in solution onto the upper (solution-facing) surface of a preexisting cluster ("piggyback" deposition) and subsequent incorporation into the cluster. Results of calculations of the time course of adsorption, carried out for two different limiting models of cluster structure and energetics, show that in the absence of piggyback deposition, enhancement of the tendency of adsorbate to cluster can reduce, but not eliminate, the negative kinetic cooperativity due to surface area exclusion by adsorbate. Apparently noncooperative (Langmuir-like) and positively cooperative adsorption progress curves, qualitatively similar to those reported in several published experimental studies, require a significant fraction of total adsorption flux through the piggyback deposition pathway. According to the model developed here and in the above-mentioned reference, the formation of surface clusters should be a common concomitant of non-site-specific surface adsorption of proteins, and may provide an important mechanism for assembly of organized "protein machines" in vivo.

INTRODUCTION

A surface may be regarded as "molecularly flat" or "planar" with respect to a particular adsorbing macromolecule if the potential of interaction between adsorbate and surface is non-site-specific, and approximately independent of adsorbate position in the plane of the surface over distances that are within one to two orders of magnitude of the characteristic length of the adsorbate molecule. Reversible non-site-specific surface adsorption of proteins is of biological interest for several reasons, including the following. 1) The interior of a cell contains a variety of membranes and other structures presenting quasi-planar surfaces to which intracellular proteins may reversibly adsorb (Minton, 1990). Such adsorption is known to be linked to the catalytic activity of several enzymes (Kurganov, 1985) and may also be linked to the formation of multienzyme complexes (Minton, 1995). 2) The process of blood coagulation depends upon membrane adsorption-linked activation of clotting factors (Walker and Krishnaswamy, 1994). 3) The adsorption of protein onto the surface of various synthetic materials (polymers, ceramics, metals) under physiological conditions may determine the biocompatibility of those materials (Andrade, 1985). Thus models for the steady-state and kinetic properties of systems containing one or more soluble proteins interacting with a molecularly flat surface can provide important insight into the behavior of proteins (and synthetic materials) in various physiological milieux.

Kinetic and equilibrium models for irreversible and reversible adsorption of proteins to planar surfaces have been developed that take into account the surface area excluded to each other by molecules of adsorbed protein (Stankowski, 1983, 1984; Schaaf and Talbot, 1989; Talbot et al., 1994; Chatelier and Minton, 1996; Talbot, 1997; Minton, 1999; Ravichandran and Talbot, 2000). In the absence of attractive interactions between molecules of adsorbed protein, these models predict that the equilibrium association "constant" and the association rate "constant" should decrease monotonically and strongly with increasing fractional surface occupancy, i.e., that equilibrium adsorption should be strongly negatively cooperative. However, it has been demonstrated experimentally that at least under some conditions, proteins may relatively rapidly and reversibly adsorb onto a variety of surfaces at fractional surface occupancies as high as that corresponding to close packing of natively structured protein (Al-Malah et al., 1995). Moreover, depending upon experimental conditions and the particular protein and surface studied, protein adsorption isotherms may indicate positive cooperativity (Cutsforth et al., 1989; Heimburg and Marsh, 1995; Nygren, 1996) and "ideal" Langmuir-like behavior (Al-Malah et al., 1995; Spaargaren et al., 1995) as well as negative cooperativity. All of these types of equilibrium isotherm may be accounted for by a recently introduced model (Minton, 2000), hereafter referred to as part I. According to the model introduced in part I, surface area exclusion by adsorbate may be compensated

Received for publication 18 May 2000 and in final form 3 January 2001.
Address reprint requests to Dr. Allen P. Minton, Laboratory of Biochemistry and Genetics, Bldg. 8, Rm. 226, National Institutes of Health, Bethesda, MD 20892-0830. Tel.: 301-496-3604; Fax: 301-402-0240; E-mail: minton@helix.nih.gov.

0006-3495/01/04/1641/08 $2.00

to a variable extent by attractive interactions between adsorbate molecules leading to reversible formation of adsorbate clusters of varying size and shape. The purpose of the present communication is to extend this equilibrium model to treat the kinetics of adsorption.

In the following section we shall briefly recapitulate the essential assumptions and results of the equilibrium model of part I. Kinetic extensions are then introduced and the resulting rate equations presented, together with a description of the procedure used to solve the rate equations numerically. Next, the results of several model-simulated adsorption processes are presented and compared qualitatively with experimental results taken from the literature.

EQUILIBRIUM MODEL FOR ADSORPTION WITH AREA EXCLUSION AND ADSORBATE CLUSTERING

The following is a condensed summary of the equilibrium model introduced and described fully in part I, reviewed here to introduce subsequently used notation. Justification for assumptions and approximations introduced into the model are presented in part I.

It is assumed that an adsorbate molecule that is monomeric and thermodynamically ideal in solution may equilibrate with adsorbed monomer according to

$$\gamma_1\rho_1 = K_1^{\mathrm{ads}}c \equiv c^* \tag{1}$$

where ρ_1 denotes the surface density of adsorbed monomer, γ_1 the activity coefficient of adsorbed monomer, K_1^{ads} the thermodynamic equilibrium constant for adsorption of monomer, c the concentration of (monomeric) adsorbate in solution, and c^* an affinity-scaled solution concentration of adsorbate. It is also assumed that adsorbed monomer may self-associate reversibly to form adsorbed oligomers denoted by species $i > 1$, where the degree of oligomerization of oligomeric species i is denoted by n_i:

$$\gamma_i\rho_i = K_{1,i}(\gamma_1\rho_1)^{n_i} \tag{2}$$

where γ_i and ρ_i denote the activity coefficient and surface density of oligomeric adsorbate species i, respectively, and $K_{1,i}$ the thermodynamic association equilibrium constant for the formation of one oligomer of species i from n_i monomers.

The activity coefficient of each adsorbed species depends upon the surface density, size, and shape of all species in a manner which is assumed to be calculable using the two-dimensional scaled particle theory of mixtures of convex hard particles (Talbot et al., 1994):

$$\ln\gamma_i(\{\rho\}) = -\ln(1-\langle\rho a\rangle) + \frac{a_i\langle\rho\rangle + s_i\langle\rho s\rangle/(2\pi)}{1-\langle\rho a\rangle} + \frac{a_i}{4\pi}\left[\frac{\langle\rho s\rangle}{1-\langle\rho a\rangle}\right]^2 \tag{3}$$

where a_i and s_i respectively denote the area and circumference of the "footprint" (projection on the plane of the surface) of adsorbed species i, and $\langle\rho\rangle \equiv \Sigma\rho_j$, $\langle\rho a\rangle \equiv \Sigma\rho_j a_j$, and $\langle\rho s\rangle \equiv \Sigma\rho_j s_j$.

Given a structural model for oligomer that specifies the size and shape of oligomer i, and the number and free energy of individual intermolecular contacts within oligomer i, the values of a_i, s_i, and $K_{1,i}$ may be calculated for all i as described in part I. Given these quantities, Eqs. 1–3 may then be solved numerically for all ρ_i and γ_i, and consequently the total amount of protein adsorbed per unit surface area ($= \Sigma n_i\rho_i$) at equilibrium as functions of c^*.

For purposes of developing a kinetic model we recast association equilibria in stepwise form. To simplify calculations we shall assume henceforth that $n_i = i$, i.e., all clusters with the same stoichiometry are structurally and energetically equivalent. Then Eq. 2 is equivalent to

$$\gamma_{i+1}\rho_{i+1} = K_{i,i+1}\gamma_i\rho_i\gamma_1\rho_1 \tag{4a}$$

and the stepwise equilibrium association constant is given by

$$K_{i,i+1} = K_{1,i+1}/K_{1,i} = \exp(-\Delta F_i/RT) \tag{4b}$$

where ΔF_i denotes the standard state free energy change associated with the addition of adsorbed monomer to i-mer, R the molar gas constant, and T the absolute temperature.

KINETIC GENERALIZATION

Adsorbate cluster growth is assumed to proceed primarily by the reversible addition of single molecules of the adsorbing species, or "monomers," to preexisting clusters. (Diffusional mobility of clusters in the plane of the surface is expected to decrease strongly with increasing cluster size, so annealing of preexisting clusters to form larger clusters is assumed at this level of approximation to contribute negligibly to overall adsorption kinetics.) The formation of i + 1-mer from i-mer and monomer in solution may proceed via two mechanistically distinct pathways, depicted schematically in Fig. 1: 1) adsorption of soluble monomer to vacant surface (elementary process 1), followed by diffusion of adsorbed monomer to the edge of cluster species i and subsequent accretion (elementary process 2). This will be referred to as the "direct deposition + accretion pathway." 2) Deposition of soluble monomer onto and insertion into cluster species i (elementary process 3). This will be referred to as the "piggyback deposition pathway."

Combination of these two pathways leads to the following set of rate equations:

$$\frac{d\rho_1}{dt} = \left[k_{1f}c + \sum_{i=1} k_{2b}^{(i)}\rho_{i+1} + (k_{2b}^{(1)} + k_{3b}^{(1)})\rho_2\right] - \left[k_{1b} + \sum_{i=1} k_{2f}^{(i)}\rho_i + k_{2f}^{(1)}\rho_1 + k_{3f}^{(1)}c\right]\rho_1 \tag{5a}$$

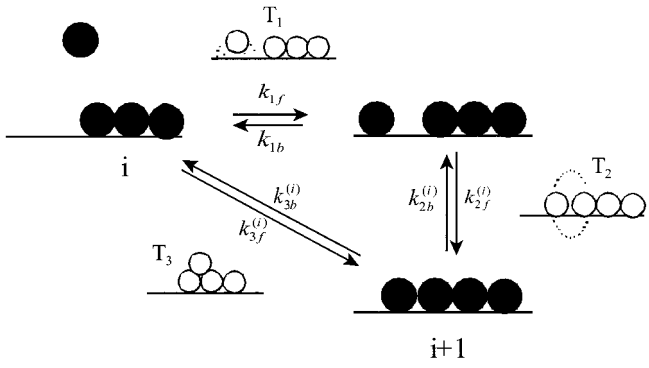

FIGURE 1 Schematic depiction of the kinetic pathways described in the text: 1) direct deposition of soluble monomer onto available surface; 2) accretion of adsorbed monomer onto cluster species i; 3) piggyback deposition of soluble monomer onto and incorporation into cluster species i.

and for $i > 1$

$$\frac{d\rho_i}{dt} = (k_{2f}^{(i-1)}\rho_1 + k_{3f}^{(i-1)}c)\rho_{i-1} + (k_{2b}^{(i)} + k_{3b}^{(i)})\rho_{i+1} - [(k_{2b}^{(i-1)} + k_{3b}^{(i-1)}) + (k_{2f}^{(i)}\rho_1 + k_{3f}^{(i)}c)]\rho_i \quad (5b)$$

Since numerical calculations will be carried out for a finite set of clusters containing a maximum of imax protomers, it follows that for i = imax, Eq. 5b reduces to

$$\frac{d\rho_{imax}}{dt} = (k_{2f}^{(imax-1)}\rho_1 + k_{3f}^{(imax-1)}c)\rho_{imax-1} - (k_{2b}^{(imax-1)} + k_{3b}^{(imax-1)})\rho_{imax} \quad (5c)$$

DEPENDENCE OF RATE COEFFICIENTS UPON CLUSTER SIZE, SHAPE, AND EXCLUDED SURFACE AREA

A general treatment of the effect of volume exclusion upon the kinetics of elementary bimolecular association and dissociation is presented in the Appendix.

Direct deposition of monomer (elementary process 1)

The transition state for this association, depicted schematically as T_1 in Fig. 1, requires near-contact approach of solute to the surface and thus corresponds to limiting case 1 of the Appendix. Hence

$$k_{1f} = k_{1f}^o/\gamma_1 \quad (6)$$

$$k_{1b} = k_{1b}^o \quad (7)$$

We note that the association rate coefficient corresponds to the product of a rate of an intrinsic rate coefficient times the probability $(1/\gamma_1)$ that the monomer hitting the surface will hit an empty region large enough to accommodate its entire footprint (Talbot et al., 1994; Minton, 1999).

Accretion of adsorbed monomer to cluster (elementary process 2)

The transition state, depicted schematically as T_2 in Fig. 1, requires near-contact approach of adsorbed monomer to the periphery of the cluster and thus corresponds again to limiting case 1 of the Appendix. Assuming that the probability of reaction is the same at any point on the periphery of cluster species i, we obtain

$$k_{2f}^{(i)} = k_{2f}^o \frac{\gamma_1\gamma_i}{\gamma_{i+1}} s_i \quad (8)$$

Combining equation 8 with equilibrium relations 4, we obtain

$$k_{2b}^{(i)} = k_{2f}^{(i)}/K_{i,i+1} = k_{2f}^{(i)}s_i/\exp(-\Delta F_i/RT) \quad (9)$$

Piggyback deposition (elementary process 3)

The transition state for this process is assumed to consist of a "piggyback complex" between monomer and the target cluster, depicted schematically as T_3 in Fig. 1. Unlike the transition states for the other two elementary processes, this transition state does not exclude additional volume to preexisting adsorbate clusters. Hence this process is an example of limiting case 2 of the Appendix, and nonideal effects resulting from area exclusion are expected to influence primarily the dissociation rather than the association rate coefficient.

The association rate is the product of two factors, the total rate R of soluble monomer hitting the surface per unit time and area, and the probability $P(i)$ that a monomer hitting the surface will land on a cluster of species i. By comparison with process 1, we write

$$R = Jk_{1f}^o c \quad (10)$$

where J is a dimensionless constant expected to be of order unity. The introduction of J allows for differences between the orientational requirements for successful adsorption onto bare surface and successful piggyback deposition on a preexisting cluster. $P(i)$ is the product of the joint probability that an approaching monomer will hit any cluster, $P_1(i)$, and the conditional probability $P_2(i)$ that a monomer hitting any cluster hits a cluster of species i. $P_1(i)$ is just 1 minus the probability that an incoming monomer hits no cluster $(1/\gamma_1)$, and P_2 is the ratio of the area covered by clusters of species i to the total area covered by all clusters $(\rho_i a_i/\Sigma\rho_j a_j)$. Thus the association rate coefficient is given by

$$k_{3f}^{(i)} = RP_1(i)P_2(i)/\rho_i = Jk_{1f}^o c(1 - 1/\gamma_1)\frac{a_i}{\sum_j \rho_j a_j} \quad (11)$$

Combining Eq. 11 with equilibrium relations 1 and 4, we obtain

$$k_{3b}^{(i)} = \frac{k_{3f}^{(i)}}{K_1^{ads}K_{i,i+1}} = \frac{Jk_{1f}^o(1 - \gamma_1^{-1})\gamma_{i+1}a_i}{\exp(-F_i/RT)K_1^{ads}\gamma_i\Sigma\rho_j a_j} \quad (12)$$

Equations 6–12 may be further simplified by scaling all rate coefficients relative to k_{1b}^o. Let $k'_X = k_X/k_{1b}^o$, where X is any subscript. Then

$$k'_{1f} = K_1^{ads}/\gamma_1 \quad (13)$$

$$k'_{1b} = 1 \quad (14)$$

$$k_{2f}^{(i)\prime} = k_{2f}^{o\prime}\frac{\gamma_1\gamma_i}{\gamma_{i+1}}s_i \quad (15)$$

$$k_{2b}^{(i)\prime} = k_{2f}^{(i)\prime}/K_{i,i+1} = k_{2f}^{o\prime}s_i/\exp(-\Delta F_i/RT) \quad (16)$$

$$k_{3f}^{(i)\prime} = JK_1^{ads}\left(1 - \frac{1}{\gamma_1}\right)\frac{a_i}{\sum_j \rho_j a_j} \quad (17)$$

$$k_{3b}^{(i)\prime} = \frac{k_{3f}^{(i)\prime}}{K_1^{ads}K_{i,i+1}} = \frac{J(1 - \gamma_1^{-1})\gamma_{i+1}a_i}{\exp(-\Delta F_i/RT)\gamma_i\Sigma\rho_j a_j} \quad (18)$$

The values of s_i, a_i, and ΔF_i appearing in the above expressions are obtained from a structural/energetic model for clusters. In the present treatment, an i-meric cluster is generally represented as a hard convex particle with footprint area equal to i times the footprint area of adsorbed monomer

$$a_i = i \times a_1, \quad (19)$$

This assumption is equivalent to assuming that all monomers in the cluster are in direct contact with the surface. The stepwise free energy of monomer addition is taken as the product of the free energy of a single inter-protomer contact times the change in the number of contacts with addition of a

monomer to an i-mer

$$\Delta F_i = \Delta n_{c,i\rightarrow i+1} U_c \tag{20}$$

In part I the circular cluster and linear cluster models were introduced as representing the most compact (least volume-excluding) and least compact (most volume-excluding) clusters possible for a given stoichiometry. The rationale for using two such highly simplified models for clusters is that even though these models are too simple to be realistic in and of themselves, one may argue with some confidence that any behavior exhibited qualitatively by both models is probably a consequence of the proposed underlying reaction mechanism in general, rather than any particular assumptions regarding cluster structure and energetics. The values of s_i and $\Delta n_{c,i\rightarrow i+1}$ obtained from these two models are given below.

Circular cluster model

Clusters have a circular footprint. For this model

$$s_i = 2(i\pi a_1)^{1/2} \tag{21}$$

The change in number of interprotomer contacts is obtained from an empirical relationship that well describes the number of contacts between circles, representing protomer, packed compactly on a hexagonal grid (part I):

$$\Delta n_{c,i\rightarrow i+1} = 2.5 + 3.78\{\exp[-(i+1)/2.51] - \exp[-i/2.51]\} \tag{22}$$

Linear cluster model

Monomer has a square footprint, and clusters are linear arrays of squares. For this model

$$s_i = 2(i+1)a_1^{1/2} \tag{23}$$

and

$$\Delta n_{c,i\rightarrow i+1} = 1 \tag{24}$$

CALCULATION OF KINETIC PROGRESS CURVES

We define the scaled time $t^* = k^o_{1b}t$. The rate equations expressed as $d\rho_i/dt^*$ are identical to Eqs. 5a–c except that all rate coefficients are replaced by the corresponding scaled quantities presented in Eqs. 13–18. Given a model for clusters that specifies the values of a_i, s_i, and $\Delta n_{c,i\rightarrow i+1}$, and user-supplied values of the adjustable parameters c^* ($= K_1^{ads}c$), $k^o_{2f}{}'$, J, and U_C, the scaled rate equations may be solved together with Eqs. 3 to yield the dependence of ρ_i and γ_i on t^*. These equations were solved for the circular and linear cluster models with $i = 1$ to 20 using the numerical differential equation solver ODE15s in MATLAB 5.3 (MathWorks, Natick, MA) with the initial condition $\rho_i(t^* = 0) = 0$ for all i. [MATLAB scripts are available upon request.] Calculated kinetic progress curves are presented as the dependence of fractional surface occupancy $\varphi(t^*) \equiv \Sigma_i \rho_i(t^*)a_i$ upon log t^*.

RESULTS AND DISCUSSION

Kinetic adsorption progress curves calculated using the models introduced here will be compared to a reference progress curve calculated according to ideal Langmuir surface binding kinetics (Langmuir, 1918), which assume the absence of any interaction (attractive or repulsive) between molecules of adsorbate:

$$\varphi(t^*) = \frac{c^*}{1+c^*}\left[1 - \exp\left(-\frac{t^*}{1+c^*}\right)\right] \tag{25}$$

To explore the kinetic contribution of each of the two alternate pathways proposed in the current model, we first present results obtained when one of the pathways is "switched off." In Fig. 2 results are shown for adsorption in the absence of piggyback deposition (cluster growth by accretion only), as calculated using the circular cluster model. The left-hand panel displays the calculated dependence of fractional surface occupancy φ on log t^*, and the right-hand panel displays the calculated dependence of adsorption rate upon φ. Curves a represent an ideal reference calculated according to Eq. 25 for the same value of c^*, and curves b–e were calculated from the circular cluster model for varying rates of accretion, with fixed equilibrium conditions and fixed rate of monomer adsorption. Salient features of these simulations are as follows.

First, when the rate of accretion is low compared to the rate of monomer adsorption (*curves a*) adsorption proceeds in two widely separated phases. The initial phase corresponds to the adsorption of monomer to a fractional surface occupancy corresponding to the equilibrium adsorption of a nonassociating monomer at solution concentration c^* (part I). The second stage of adsorption corresponds to additional adsorption of monomer at a much slower rate, which is limited by the amount of free surface area (Fig. 3).

Second, as the rate of accretion becomes larger the adsorption progress curve approaches an asymptotic limit (*curve e* in Fig. 2) in which all surface clusters are in instantaneous chemical equilibrium, and the overall rate of adsorption at any time depends upon the fraction of surface area made available for additional monomer adsorption by the equilibrium distribution of clusters at that time. It is

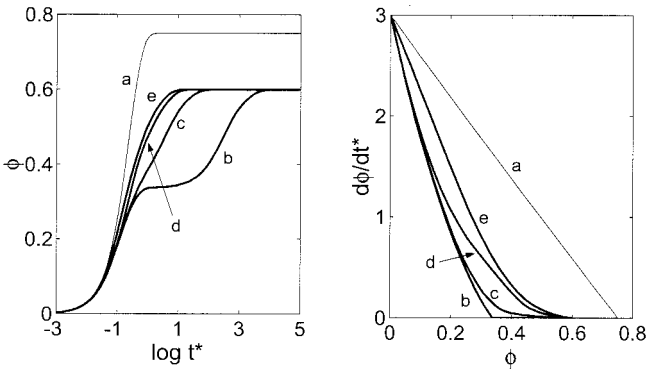

FIGURE 2 Kinetics of adsorption via the direct deposition + accretion pathway, calculated for the circular cluster model. *Curves a* are reference curves representing Langmuirian kinetics calculated according to Eq. 25 with $c^* = 3$. Simulation parameters: $c^* = 3$, $U_c = 0$, $J = 0$ throughout, and $k^o_{2f} = 0.001$ (*curves b*), 0.1 (*c*), 1 (*d*), and 1000 (*e*).

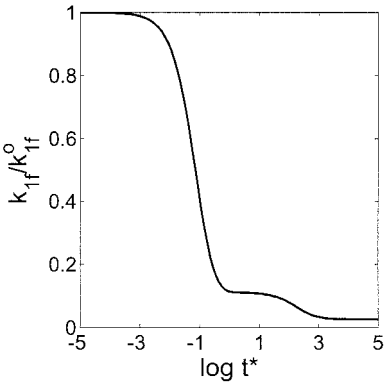

FIGURE 3 Time dependence of the rate of direct deposition, calculated for the simulation shown in Fig. 2, *curves b*.

evident upon inspection of the right-hand panel of Fig. 2 that in the absence of direct deposition, the rate of adsorption will always be less than the ideal (exponential) rate of adsorption because of decreasing available area for adsorption of additional monomer. The upward concave shape of the curve of $d\varphi/dt^*$ is a reflection of negative kinetic cooperativity, i.e., a condition in which occupancy of some fraction of the surface by adsorbate decreases the effective rate coefficient for subsequent adsorption.

The results of comparable calculations carried out on the linear cluster model are shown in Fig. 4. It is evident that the linear and circular cluster models yield qualitatively similar behavior, the main difference arising from the different levels of equilibrium adsorption of circular and linear clusters.

In Fig. 5 calculated results are shown for adsorption in the absence of accretion (cluster growth via piggyback deposition only), as calculated using the circular cluster model. When the rate of piggyback deposition is very small relative to the rate of direct deposition of monomer (*curves b*), adsorption becomes biphasic; the faster phase corresponds to the adsorption of nonassociating monomer, followed by growth of clusters at a much slower rate. This kinetic

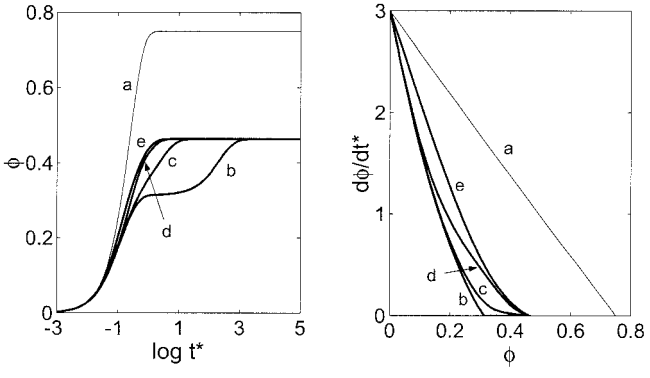

FIGURE 4 Kinetics of adsorption via the direct deposition + accretion pathway, calculated for the linear cluster model. Parameter values are as given in the caption to Fig. 2.

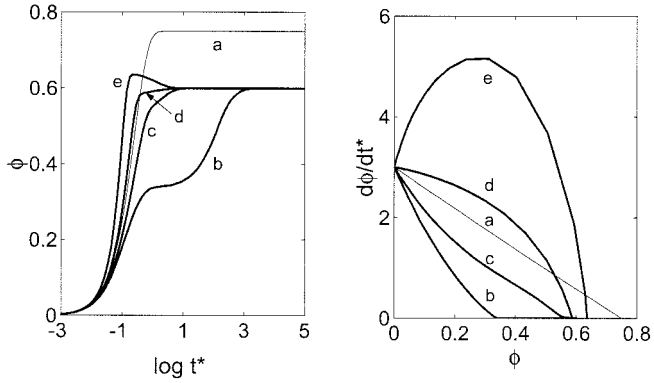

FIGURE 5 Kinetics of adsorption via the piggyback deposition pathway, calculated for the circular cluster model. *Curves a* are reference curves representing Langmuirian kinetics calculated according to Eq. 25 with $c^* = 3$. Simulation parameters: $c^* = 3$, $U_c = 0$, $k^o_{2f} = 0$ throughout, and $J = 0.001$ (*curves b*), 0.3 (*c*), 1.0 (*d*), and 3.0 (*e*).

behavior closely resembles that of the accretion-only pathway, in the limit that accretion occurs over a much larger time scale than monomer deposition (cf. *curves b* of Fig. 2). The difference between the kinetic contribution of the two pathways becomes evident at higher rates of piggyback deposition. With increasing rate of monomer deposition, the adsorption progress curves steepens, first approaching the exponential behavior exhibited by the ideal adsorption curve (*curves c*), and then becoming even steeper (*curves d*), ultimately achieving a condition in which the rate of adsorption actually increases with increasing fractional occupancy at lower levels of surface occupancy (*curves e*). At the highest rate of deposition a small degree of kinetic overshoot is apparent. The upwardly convex shapes of *curves d* and *e* in the right-hand panel of Fig. 5 are indicators of positive kinetic cooperativity, i.e., a condition in which occupancy of some fraction of the surface by adsorbate increases the effective rate coefficient for subsequent adsorption.

The results of comparable calculations carried out on the linear cluster model are shown in Fig. 6. As in the case of the accretion pathway calculations summarized in Figs. 2 and 4, the linear and circular cluster models yield qualitatively similar behavior, the main difference arising from the different levels of equilibrium adsorption of circular and linear clusters.

Under circumstances such that the rate of direct deposition per unit area of cluster was comparable to the rate of monomer adsorption per unit area of available free surface, the overall rate of adsorption would be expected to be insensitive to the fractional occupancy of surface, and that under such conditions one might observe quasi-exponential adsorption kinetics. In Fig. 7 an example is presented of a calculated adsorption progress curve exhibited by a highly nonideal system that displays almost perfectly exponential adsorption kinetics. In the absence of additional data, an

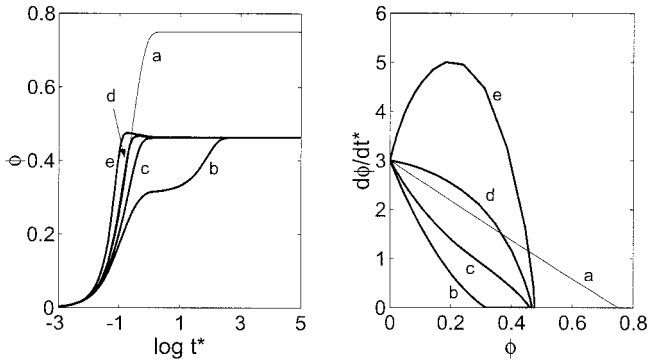

FIGURE 6 Kinetics of adsorption via the piggyback deposition pathway, calculated for the linear cluster model. Parameter values are as given in the caption to Fig. 5.

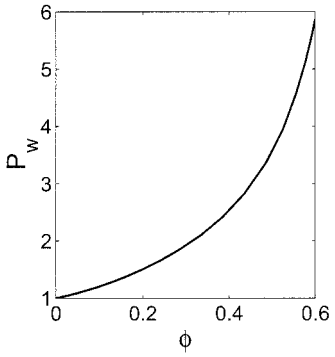

FIGURE 8 Weight-average degree of cluster polymerization P_w, calculated from the simulation of Fig. 7, plotted as a function of fractional surface occupancy φ.

investigator observing such time dependence might attribute it to the lack of interaction between molecules of adsorbate. However, the weight-average degree of adsorbate oligomerization (cluster size), calculated from this model according to

$$P_w(t^*) \equiv \frac{\sum_i i^2 \rho_i(t^*)}{\sum_i i \rho_i(t^*)} \tag{26}$$

increases substantially with increasing fractional surface occupancy, as shown in Fig. 8. The observed kinetics should properly be termed "pseudo-Langmuirian" rather than "quasi-Langmuirian," as the latter term connotes near-absence of interadsorbate interactions rather than the reality of substantial but compensating attractive and repulsive interactions.

The experimental literature on kinetics of protein adsorption contains examples of negative kinetic cooperativity (Ramsden, 1993; Ramsden et al., 1994; Wahlgren et al., 1995), quasi- or pseudo-Langmuirian kinetics (Ramsden et al., 1994; Spaargaren et al., 1995), and positive kinetic cooperativity (Nygren, 1993, 1994; Ball and Ramsden, 1997). Previous models taking into account the effect of excluded surface area on adsorption kinetics (Talbot et al., 1994; Sild et al., 1996; Minton, 1999; Ravichandran and Talbot, 2000) have focused exclusively on direct deposition of monomer, neglecting clustering and hence the possibility of piggyback deposition. The present treatment indicates that in the absence of piggyback deposition, cluster formation can reduce but not eliminate the negative kinetic cooperativity arising from area exclusion by adsorbate. The present model predicts that pseudo-Langmuirian or positively cooperative adsorption progress curves are possible only when a substantial fraction of total adsorption proceeds via piggyback deposition of monomer on existing clusters.

To the best of the author's knowledge, the kinetic model presented here is the only quantitative mechanistic model so far proposed that can account for the experimentally observed positive kinetic cooperativity cited above, and it is the only model that can account for Langmuir-type adsorption kinetics when the surface density of adsorbate approaches that of a two-dimensional close-packed array of adsorbate in the limit of long time. Until now, almost all quantitative studies of protein adsorption kinetics have been carried out using techniques that monitor the average amount of protein adsorbed per unit surface area as a function of time. Using techniques such as electron microscopy or atomic force microscopy, it may be possible to directly observe clusters of adsorbed protein if and when they are present (see, for example, Nygren and Stenberg, 1990; Schwartz et al., 1992), and to quantify cluster size and shape distribution as a function of the time of exposure of the surface to supernatant protein solution.

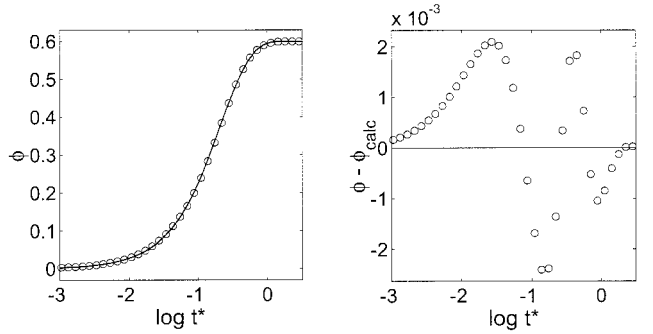

FIGURE 7 (*Left*) Points: calculated adsorption progress curve for circular cluster model with $c^* = 3$, $U_c = 0$, $k^o_{2f} = 10$, $J = 0.4$. *Curve*: best least-squares fit of Eq. 25 (Langmuir kinetics). (*Right*) Difference between circular cluster model simulation and best fit of single exponential to results shown in the left-hand panel.

APPENDIX

Effect of volume exclusion on the rate of an elementary bimolecular association reaction in the transition-state limit

We consider the association of species i and j to form the bimolecular complex ij. In accordance with simple transition-state rate theory (Hill,

1960), it is assumed that the rate of association is equal to the rate with which an encounter or transition-state complex T, in pseudo-equilibrium with reactants i and j, decays to the final association product ij.

$$\text{association rate} = k_{T\rightarrow ij}\rho_T \tag{A1}$$

where ρ_T is a steady-state concentration of transition state. Since the equilibrium concentration of T is given by

$$\gamma_T\rho_T = K_{i+j,T}\gamma_i\rho_i\gamma_j\rho_j \tag{A2}$$

equation A1 may be rewritten

$$\text{association rate} = k_F\rho_i\rho_j \tag{A3}$$

where

$$k_F = k_{T\rightarrow ij}K_{i+j,T}\frac{\gamma_i\gamma_j}{\gamma_T} = k_F^o\frac{\gamma_i\gamma_j}{\gamma_T} \tag{A4a}$$

In an entirely analogous fashion it may be shown that the rate constant for the dissociation reaction is given by

$$k_B = k_B^o\frac{\gamma_{ij}}{\gamma_T} \tag{A4b}$$

It is emphasized that relations (A4) are expected to hold only for transition-state rate-limited association reactions, i.e., when the rate of formation of complex is much slower than the rate of bimolecular encounter. We shall refer to k_F^o and k_B^o as rate constants, and k_F and k_B as rate coefficients, since it is evident that the concentrations of reactant and product will in general vary with time, and depending upon the absolute magnitudes of these concentrations, the ratios of activity coefficients appearing in Eqs. A4, and hence k_F and k_B, may likewise vary substantially with time. Let us consider two limiting cases of the general relations (A4).

Limiting case (1)

The transition-state complex excludes approximately the same volume to other macrosolutes as does the fully formed complex. In this limit $\gamma_T \approx \gamma_{ij}$, and Eqs. A4 reduce to

$$k_F \approx k_F^o\frac{\gamma_i\gamma_j}{\gamma_{ij}} \tag{A5a}$$

and

$$k_B \approx k_B^o \tag{A5b}$$

Under these conditions, volume exclusion affects primarily the association rate coefficient.

Limiting case (2)

The transition-state complex excludes approximately the same volume to other macrosolutes as do the separated reactants. In this limit $\gamma_T \approx \gamma_i\gamma_j$, and Eqs. A4 reduce to

$$k_F \approx k_F^o \tag{A6a}$$

and

$$k_B \approx k_B^o\frac{\gamma_{ij}}{\gamma_i\gamma_j} \tag{A6b}$$

Under these conditions, volume exclusion affects primarily the dissociation rate coefficient. For most types of association reactions, limiting case (1) would be expected to be a more realistic approximation (Minton, 1983). However, an example of limiting case (2) will be encountered in the models described in the text.

The author thanks Prof. G. J. Howlett and the University of Melbourne for a Visiting Research Scholarship (May–August 1999) during which the present study was carried out. I also thank faculty and staff of the Russell Grimwade School of Biochemistry, and members of the Howlett and Sawyer laboratories in particular, for their warm hospitality, and Drs. Peter Schuck, NIH, and Julian Talbot, Duquesne Univ., for helpful comments on the first draft of this paper.

REFERENCES

Al-Malah, K., J. McGuire, and R. Sproull. 1995. A macroscopic model for the single-component protein adsorption isotherm. *J. Colloid Interface Sci.* 170:261–268.

Andrade, J. D. 1985. Surface and Interfacial Aspects of Biomedical Polymers, Vol. 2. Protein Adsorption. Plenum, New York.

Ball, V., and J. J. Ramsden. 1997. Absence of surface exclusion in the first stage of lysozyme adsorption is driven through electrostatic self-assembly. *J. Phys. Chem. B.* 101:5465–5469.

Chatelier, R. C., and A. P. Minton. 1996. Adsorption of globular proteins on locally planar surfaces: models for the effect of excluded surface area and aggregation of adsorbed protein on adsorption equilibria. *Biophys. J.* 71:2367–2374.

Cutsforth, G. A., R. N. Whitaker, J. Hermans, and B. R. Lentz. 1989. A new model to describe extrinsic protein binding to phospholipid membranes of varying composition: application to coagulation proteins. *Biochemistry.* 28:7453–7461.

Heimburg, T., and D. Marsh. 1995. Protein surface distribution and protein-protein interactions in the binding of peripheral proteins to charged lipid membranes. *Biophys. J.* 68:536–546.

Hill, T. L. 1960. Introduction to Statistical Thermodynamics, Chap. 11. Addison-Wesley, Reading, MA.

Kurganov, B. I. 1985. Control of enzyme activity in reversibly adsorptive enzyme systems. *In* Organized Multienzyme Systems. G. R. Welch, editor. Academic Press, Orlando, FL. 241–270.

Langmuir, I. 1918. The adsorption of gases on plane surfaces of glass, mica and platinum. *J. Am. Chem. Soc.* 40:1361–1402.

Minton, A. P. 1983. The effect of volume occupancy upon the thermodynamic activity of proteins: some biochemical consequences. *Mol. Cell. Biochem.* 55:119–140.

Minton, A. P. 1990. Holobiochemistry: an integrated approach to the understanding of biochemical mechanisms that emerges from the study of proteins and protein associations in volume-occupied solutions. *In* Structural and Organizational Aspects of Metabolic Regulation. P. A. Srere, M. E. Jones, and C. K. Mathews, editors. Alan R. Liss, New York. 291–306.

Minton, A. P. 1995. Confinement as a determinant of macromolecular structure and reactivity. II. Effects of weakly attractive interactions between confined macrosolutes and confining structures. *Biophys. J.* 68:1311–1322.

Minton, A. P. 1999. Adsorption of globular proteins on locally planar surfaces. II. Models for the effect of multiple adsorbate conformations on adsorption equilibria and kinetics. *Biophys. J.* 76:176–187.

Minton, A. P. 2000. Effects of excluded surface area and adsorbate clustering on surface adsorption of proteins. I. Equilibrium models. *Biophys. Chem.* 86:239–247.

Nygren, H. 1993. Nonlinear kinetics of ferritin adsorption. *Biophys. J.* 65:1508–1512.

Nygren, H. 1994. Kinetics of antibody binding to surface-immobilized antigen. Analysis of data and an empiric model. *Biophys. Chem.* 52: 45–50.

Nygren, H. 1996. Attractive adsorbate interaction in biological surface reactions. *Biophys. Chem.* 61:73–84.

Nygren, H., and M. Stenberg. 1990. Surface-induced aggregation of ferritin: kinetics of adsorption to a hydrophobic surface. *Biophys. Chem.* 38:67–75.

Ramsden, J. J. 1993. Concentration scaling of protein deposition kinetics. *Phys. Rev. Lett.* 71:295–298.

Ramsden, J. J., G. I. Bachmanova, and A. I. Archakov. 1994. Kinetic evidence for protein clustering at a surface. *Phys. Rev. E.* 50:5072–5076.

Ravichandran, S., and J. Talbot. 2000. Mobility of adsorbed proteins: a Brownian dynamics study. *Biophys. J.* 78:110–120.

Schaaf, P., and J. Talbot. 1989. Surface exclusion effects in adsorption processes. *J. Chem. Phys.* 91:4401–4409.

Schwartz, D. K., S. Steinberg, J. Israelachvili, and J. A. N. Zasadzinski. 1992. Growth of a self-assembled monolayer by fractal aggregation. *Phys. Rev. Lett.* 69:3354–3357.

Sild, V., J. Ståhlberg, G. Pettersson, and G. Johansson. 1996. Effect of potential binding site overlap to binding of cellulase to cellulose: a two-dimensional simulation. *FEBS Lett.* 378:51–56.

Spaargaren, J., P. L. A. Giesen, M. P. Janssen, J. Voorberg, G. M. Willems, and J. A. vanMourek. 1995. Binding of blood coagulation factor VIII and its light chain to phosphatidylserine/phosphatidylcholine bilayers as measured by ellipsometry. *Biochem. J.* 310:539–545.

Stankowski, S. 1983. Large-ligand adsorption to membranes. II. Disk-like ligands and shape-dependence at low saturation. *Biochim. Biophys. Acta.* 735:352–360.

Stankowski, S. 1984. Large-ligand adsorption to membranes. III. Cooperativity and general ligand shapes. *Biochim. Biophys. Acta.* 777:167–182.

Talbot, J. 1997. Molecular thermodynamics of binary mixture adsorption: a scaled particle theory approach. *J. Chem. Phys.* 106:4696–4706.

Talbot, J., X. Jin, and N.-H. L. Wang. 1994. New equations for multicomponent adsorption kinetics. *Langmuir.* 10:1663–1666.

Wahlgren, M., T. Arnebrant, and I. Lundstron. 1995. Adsorption of lysozyme to hydrophilic silicon oxide surfaces: comparison between experimental data and models for adsorption kinetics. *J. Colloid Interface Sci.* 175:506–514.

Walker, R. K., and S. Krishnaswamy. 1994. The activation of prothrombin by the prothrombinase complex. Contribution of the substrate-membrane interaction to catalysis. *J. Biol. Chem.* 269:27441–27450.